International Journal of Fluid Machinery and Systems
Vol. 6, No. 3, July-September 2013

DOI: http://dx.doi.org/10.5293/IJFMS.2013.6.3.137
ISSN (Online): 1882-9554

Original Paper (Invited)

Application of Constant Rate of Velocity or Pressure Change Method to Improve Annular Jet Pump Performance

Xuelong Yang[1,2], Xinping Long[1,2], Yong Kang[1,2] and Longzhou Xiao[1,2]

[1]School of Power and Mechanical Engineering, Wuhan University
No.8 Donghu South Road, Wuhan, 430072, China
[2]Key Laboratory of Hubei Province for Water Jet Theory &New Technology, Wuhan University
No.8 Donghu South Road, Wuhan, 430072, China
xuelongge@126.com, xplong@whu.edu.cn, kangyong@whu.edu.cn, lzxiao@whu.edu.cn

Abstract

To improve annular jet pump (AJP) performance, new ways named constant rate of velocity/pressure change method (CRVC/CRPC) were adopted to design its diffuser. The design formulas were derived according to the assumption of linear velocity/pressure variation in the diffuser. Based on the two-dimensional numerical simulations, the effect of the diffuser profile and the included angle on the pump performance and the internal flow details has been analyzed. The predicted results of the RNG k-epsilon turbulence model show a better agreement with the experiment data than that of the standard and the realizable k-epsilon turbulence models. The AJP with the CRPC diffuser produces a linear pressure increase in the CRPC diffuser as expected. The AJP with CRPC/CRVC diffuser has better performance when the diffuser included angle is greater or the diffuser length is shorter. Therefore, the AJP with CRPC/CRVC diffuser is suitable for applications requiring space limitation and weight restriction.

Keywords: Jet pump, turbulence model, annular jet pump, diffuser, numerical simulation, structure optimization.

1. Introduction

A jet pump is a device utilizing kinetic energy of the primary flow to drive the secondary or induced flow by turbulent mixing. In general, there are two types of jet pumps: center jet pump (CJP) and annular jet pump (AJP). The former one has a primary jet nozzle placed along the centerline of the pump and the secondary stream flows around it annularly. While the AJP has the suction chamber placed in the center and the outside annular driving jet flows around the suction stream. The geometry of the AJP makes it well suitable for applications in the hydraulic transport of large solids. The typical usage of such pump is the transporting of live fish, large cylindrical capsules, food products, etc. [1].

Several investigations have been carried out to study the effect of pump geometry on its performance and flow details e.g. the area ratio of annular nozzle to throat, the reducing angle of the suction chamber, the throat length [1-4]. However, investigation of the influence of diffuser profile on the pump performance is lacking.

Traditionally, the diffuser profile is conical. However, the trumpet-shaped diffusers designed by constant rate of velocity/pressure change (CRVC/CRPC) method provided markedly higher efficiencies than the conical diffusers of the same length and outlet-to-inlet area ratio [5]. Therefore, a trumpet-shaped diffuser may be worth considering for performance improvement of the annular jet pump [6]. Because the trumpet-shaped diffuser is relatively difficult to be manufactured, experiment investigations on the annular jet pump with trumpet-shaped diffusers are less reported.

For many years, the computational fluid dynamics (CFD) technique has proved to be an efficient tool for flow field analysis and performance predictions of the AJP [3, 4, 7, 8]. This paper therefore adopts the CFD technique to predict the performance of the AJP with the CRVC/CRPC diffusers. The diffuser included angle is also changed to coordinate with the new diffuser profiles.

2. Models and validation of flow simulation

2.1 CFD Model

Shimizu et al. [2] has investigated experimentally the relation between configuration and performance of the annular type jet pump. In Shimizu et al.'s experiment [2], driving water supplied by a centrifugal pump flowed into a rectifying chamber via the flow

Received June 21 2013; revised January 20 2013; accepted for publication February 28 2013: Review conducted by Prof. Hyung-Hee Cho. (Paper number O13008S)
Corresponding author: Xinping Long, Professor, xplong@whu.edu.cn

measuring orifice. It then discharged from the annular nozzle (Fig. 1) outside of the central suction nozzle. The suction line consisted of the suction pipe, electro-magnetic flow meter, and suction nozzle. Driving water and entrained water mixed together in the suction chamber and flowed out from the delivery line after recovering pressure in a diffuser. Twenty-five pumps of different structure combinations were tested in the experiments. These pumps reached a maximum efficiency of thirty-six percent. The pump with the maximum efficiency was chosen as the model pump to be improved in this work. The configuration and dimensions of the chosen AJP is shown in Fig. 1 and Table 1. The AJP performance is usually described in terms of volumetric flow ratio M, total pressure ratio N, and efficiency η as defined in the nomenclature.

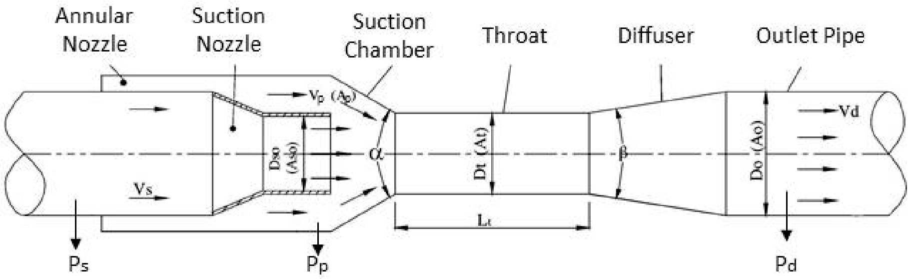

Fig. 1 Configuration of the annular jet pump from Shimizu et al. [2]

Table 1 Pump dimensions

Symbol	D_0 /mm	D_{s0} /mm	D_t /mm	L_t /mm	α /°	β /°
Dimension	55	43	38	102.3	30	5.8

The flow inside the AJP was assumed as axisymmetric flow and the CFD model was therefore simplified as two-dimension one. The axisymmetric solver was applied to take the three-dimension (3-D) effect into account in this work. The models and structured meshes are shown in Fig. 2. The length of the inlet section was 1 D_{s0} and the length of the outlet pipe was chosen as 3 D_0. The length of the outlet pipe is slightly longer than the real one, because extending properly the length of the outlet pipe is helpful to the calculation stability. Other parameters were exactly the same as those used in the experiment [1].

The flow inside the pump was assumed to be steady and incompressible flow, controlled by the Reynolds averaging Navier Stokes equations and the continuity equation. In this study, the three frequently-used k-epsilon turbulence models (the standard, realizable and RNG model) were selected to govern the turbulence characteristics with the standard wall function adopted to resolve the near-wall region. In the simulation, velocity boundary conditions were applied on the inlets boundaries and pressure boundary condition on the outlet boundary. The governing equations were discreted by the finite volume method and the secondary upwind scheme was adopted for spatial discretization of the convection terms. The SIMPLE algorithm was employed to solve the coupling the pressure and velocity.

The grid number was initially made at about 35 thousand and later increased to about 60 thousand to confirm that the results were grid independent. The maximum wall y+ value was around 120 and for most of the wall regions, y+ was around 40.

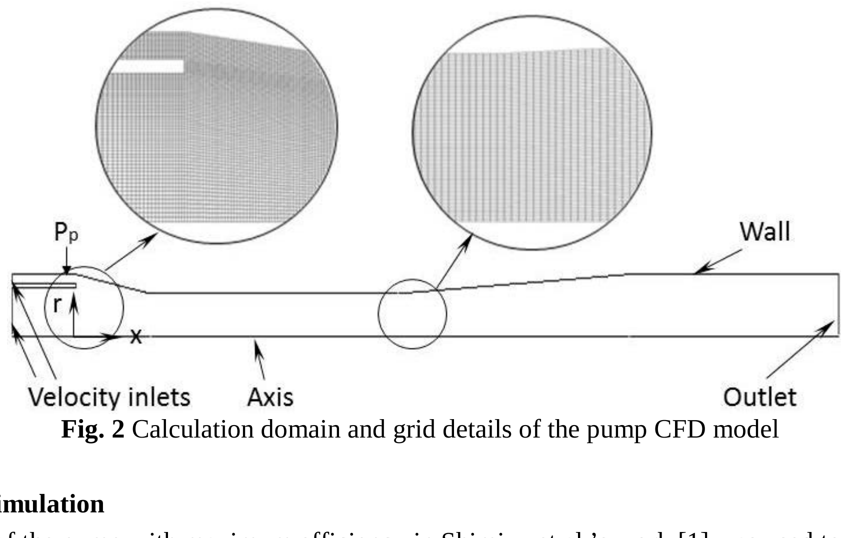

Fig. 2 Calculation domain and grid details of the pump CFD model

2.2 Validation of CFD Simulation

The experiment data of the pump with maximum efficiency in Shimizu et al.'s work [1] was used to validate the CFD results. The experimentally tested pump achieved its peak efficiency at M=0.58 and then the efficiency droped rapidly beyond this point due to the cavitation. The pumps usually worked at non-cavitation conditions, hence, the simulated working condition reached to M=0.58 only. Due to the large inlet velocity, the pressure of the primary flow decreased quickly, so the location of the primary flow pressure was important and it was obtained exactly the same as that in the experiment (Fig. 2). While the locations of the secondary flow pressure and the outlet pressure were less important because the velocity of these flows were lower.

Comparisons among the numerical results and the experimental data were shown in Fig. 3. Trends of the numerical results match well with the experiment for the efficiency η varied with flow ratio M. It can be seen from Fig. 3 that the calculated efficiency by the three models agree well with the experiment data at smaller flow ratio M but the agreement of the standard and realizable models deteriorates as M increases. The results of the RNG model are in good agreement with the experiment at the peak efficiency, while those of the other two models have obvious discrepancies. The comparison shows that the RNG k-epsilon model gives the best prediction for both trend and peak efficiency. This conclusion can also be found in Kwon et al.'s work [3]. Therefore, the RNG model is adopted in the following work.

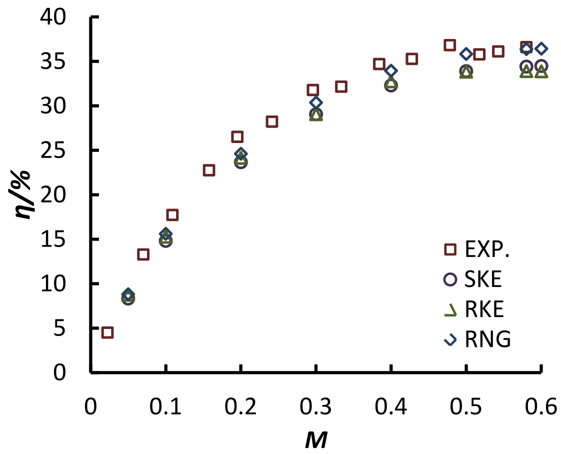

Fig. 3 Comparison of AJP performance between experiment data and CFD results

3. CRVC/CRPC Method

3.1 Description of CRVC Method

The CRVC method produces a diffuser profile that generates uniform velocity gradient allowing the velocity to rise linearly from the inlet to the outlet of the diffuser. The method is based on the following assumption,

$$\frac{\mathrm{d}v}{\mathrm{d}x} = k\,, \tag{1}$$

where k is a constant and v is mean velocity at diffuser inlet.

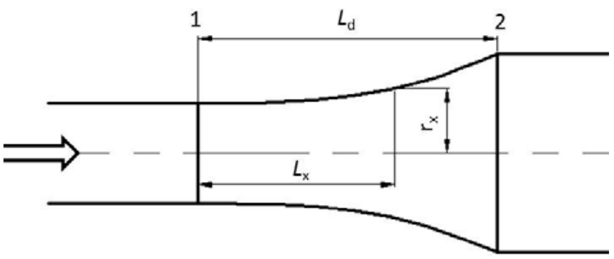

Fig. 4 Geometry of a CRPC diffuser

Referring to Fig.4, the boundary conditions for eq. (1) are v_x=v_1 at L_x=0 and v_x=v_2 at L_x = L_d. Therefore, eq. (1) can be expressed as

$$v_x - v_1 = \frac{v_2 - v_1}{L_d} L_x\,. \tag{2}$$

Because v=Q/A, and the flow rate Q keeps the same at all sections of the diffuser. Therefore eq. (2) can be expressed as

$$\frac{1}{A_x} - \frac{1}{A_1} = \frac{L_x}{L_d}\left(\frac{1}{A_2} - \frac{1}{A_1}\right). \tag{3}$$

Because $A=\pi r^2$, so eq. (3) can be converted as

$$r_x^{-2} - r_1^{-2} = \frac{L_x}{L_d}\left(r_2^{-2} - r_1^{-2}\right). \tag{4}$$

3.2 Description of CRPC method

The CRPC method produces a diffuser profile that generates uniform pressure gradient and allows the static pressure to rise linearly from the inlet to the outlet of the diffuser. The method is based on the following assumption,

$$\frac{\mathrm{d}p}{\mathrm{d}x} = k\,, \tag{5}$$

where k is a constant. Referring to Fig.4, the boundary conditions for eq. (5) are $p_x=p_1$ at $L_x=0$ and $p_x=p_2$ at $L_x = L_d$. Therefore, eq. (5) can be expressed as

$$p_x - p_1 = \frac{p_2 - p_1}{L_d} L_x \,. \tag{6}$$

Assuming that the total pressure P remains constant in the diffuser, then

$$p = P - \frac{1}{2}\rho v^2 \,. \tag{7}$$

Therefore,

$$\frac{\mathrm{d}p}{\mathrm{d}x} = -\frac{\mathrm{d}\left(v^2\right)}{\mathrm{d}x} = k \,. \tag{8}$$

Equation (8) implies that the CRPC method could make the square of the mean velocity (or the velocity head) fall linearly downstream the diffuser. Then the eq. (6) can be expressed as

$$v_x{}^2 - v_1{}^2 = \frac{v_2{}^2 - v_1{}^2}{L_d} L_x \,. \tag{9}$$

Because $v=Q/A$, and the flow rate Q is the same at all sections of the diffuser. Therefore Eq. (9) can be expressed as

$$\frac{1}{A_x{}^2} - \frac{1}{A_1^2} = \frac{L_x}{L_d}\left(\frac{1}{A_2{}^2} - \frac{1}{A_1^2}\right). \tag{10}$$

Because $A=\pi r^2$, so eq. (10) can be converted as

$$r_x^{-4} - r_1^{-4} = \frac{L_x}{L_d}\left(r_2^{-4} - r_1^{-4}\right). \tag{11}$$

Once r_1, r_2 and L_d are known, the trumpet-shaped diffuser profile could be obtained according to eq. (4) and eq. (11). Fig.5 shows the CRVC/CRPC diffuser profile compared with the conical diffuser of the original jet pump. The CRVC/CRPC diffuser has the same length and outlet-to-inlet area ratio with the conical angle. The CRVC/CRPC diffuser provides a lower rate of area change in the diffuser inlet section but a greater included angle at outlet section and its diameter is smaller than the conical diffuser at the same axial position.

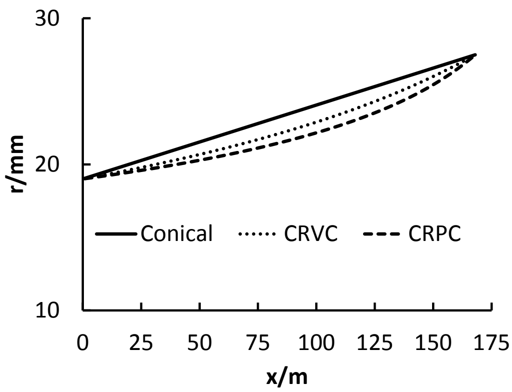

Fig. 5 Diffuser profiles

4. Results and discussion

4.1 Effect of the geometry on the AJP performance

The curves of efficiency versus flow ratio are depicted in Fig.6. CO, CV and CP in the following figures stand for the three diffuser profiles: conical, CRVC and CRPC; the value 8 and 5.8 means the included angle of the conical diffuser. Because the CRVC and CRPC diffuser is designed based on the conical diffuser, the included angle β of the corresponding conical diffuser is also defined as the nominal included angle of the CRVC and CRPC diffuser. The efficiency of the pump with CRVC/CRVC diffusers is higher than the original pump at large flow ratio ($M\geq0.4$) as β =5.8°; The performance of the AJP with CRPC diffuser is better than that with the CRVC diffuser at large flow ratio ($M\geq0.5$) but worse at small flow ratio. The larger flow ratio means bigger radial velocity gradient and needs longer throat to have the two flows well-mixed, so the unwell-mixed flow due to the short throat provides non-uniform velocity distribution at the diffuser inlet, thus causes greater hydraulic losses in the diffuser. The CRVC/CRPC diffusers which provide a low rate of area variation in the diffuser inlet section, permit mixing to be completed more efficiently.

As described in reference [4], the AJP with the trumpet-shaped diffusers presents higher performance with greater β or shorter diffuser length. Therefore the efficiency of the AJPs of β =8°were also compared as shown in Fig. 6. In general, the AJPs with CRVC/CRPC diffuser have better performance than the pumps with conical diffuser as β =8°.

The diameter of the CRVC/CRPC diffuser is smaller than that of the conical diffuser at the same axis location. This will results in greater friction loss. When the flow ratio is small, the velocity distribution at the diffuser inlet is relatively uniform and the advantage of low rate of area change is useless and counteracted by the greater friction loss. Hence, the conical diffuser has the highest efficiency at the smallest flow ratio.

The interaction between the included angle and profile makes the AJP with CRVC/CRPC diffusers of β of 8°own more stable and better performance than that of the AJPs with both trumpet-shaped or conical diffuser of β of 5.8°. Thus, the trumpet-shaped diffuser is better when its included angle is greater or the length is shorter. Therefore, the CRVC/CRPC diffuser is suitable for applications requiring space limitation and weight restriction.

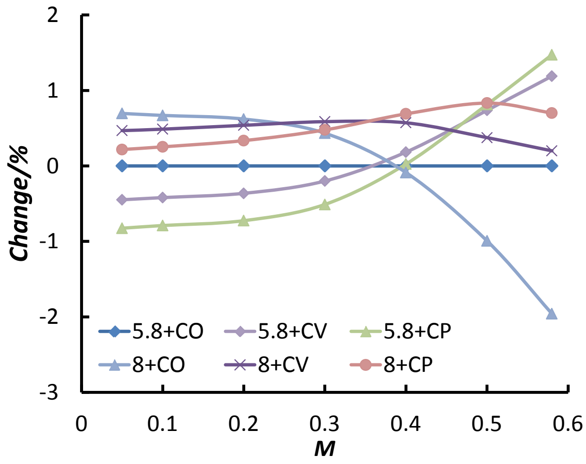

Fig. 6 Comparison of AJP efficiency change

4.2 Effect of the geometry on the flow details

The wall static pressure coefficient C_p along the pump wall is depicted in Fig.7. All the illustrations in this section are obtained at M=0.58. Due to the large velocity of the primary flow, p_p decreases considerably before entering the suction chamber. Thus, the length and diameter of the inlet straight pipe should be carefully considered to avoid larger friction loss. The pressure drops steeply in the suction chamber but varies smoothly in the throat. Then, the mixed flow enters the diffuser and obtains its major pressure recovery as shown in Fig.7.

The CRPC diffuser produces a linear pressure increase as expected. Both the CRPC and CRVC diffuser creature a smoother and more uniform pressure gradient than the conical diffuser.

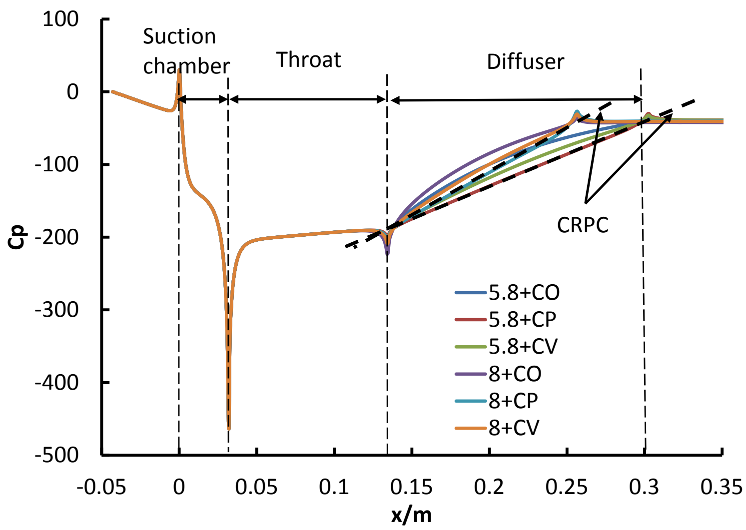

Fig. 7 Wall pressure coefficient distributions

Figure 8 shows the variation of velocity at centerline along the AJP axis. The axial velocity increases steeply in the suction chamber and then decreases slowly in the throat. In the CRVC diffusers, the axis velocity variation appears nonlinear and inconsistent with the assumption in eq. (1), because the flows are not well-mixed and the velocity distributions at diffuser inlet are not uniform (Fig.9). The CRPC/CRVC diffuser produces a more uniform velocity gradient than the conical diffuser as β=8°.

The velocity profiles and the modified coefficient of momentum λ at the diffuser inlet and outlet are depicted in Fig.9. λ defined in eq. (12) is used to weight the uniformity of the velocity distribution at the diffuser inlet (throat outlet) and the diffuser outlet.

$$\lambda = \frac{1}{Av^2}\int_A u^2 dA \tag{12}$$

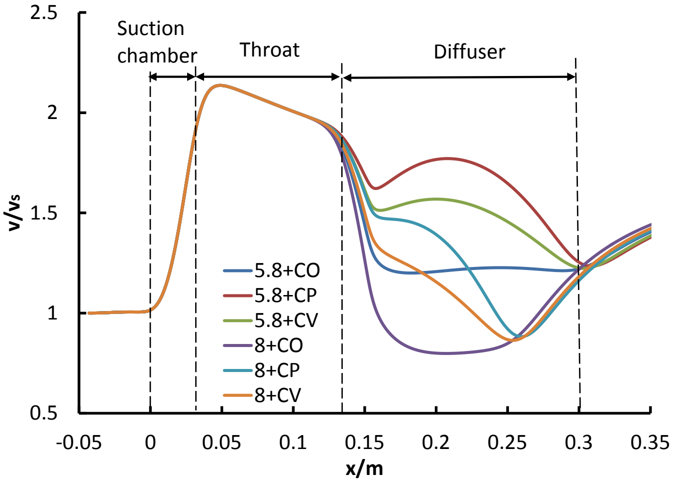

Fig. 8 Axis velocity along AJP axis

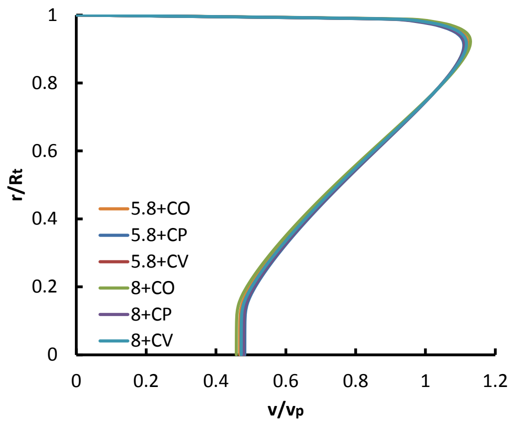

a. Velocity profiles at diffuser inlet

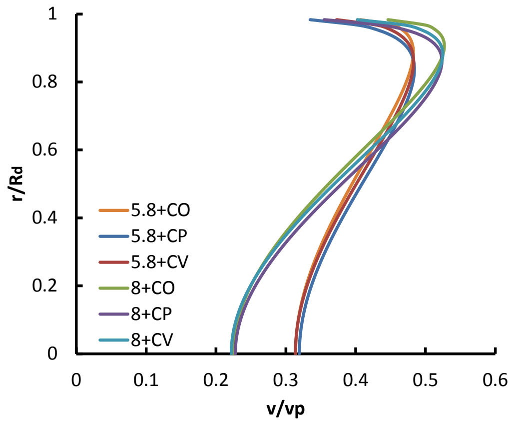

b. Velocity profiles at diffuser outlet

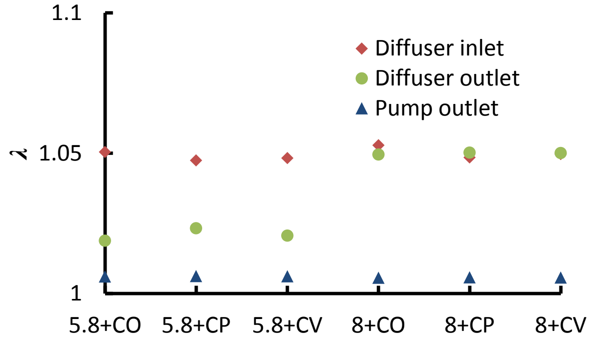

c. λ at diffuser inlet and outlet

Fig. 9 Velocity profiles and λ at diffuser inlet and outlet

The velocity profiles and λ at the diffuser inlet plotted in Fig.9a and Fig.9c are mainly affected by the throat length and have no connection with the diffuser geometry. The longer the throat is, the more uniformly the velocity distributes at the diffuser inlet, but over-long throat causes great friction loss [3].

The velocity profile and λ at diffuser outlet illustrated in Fig.9b and Fig.9c are affected by diffuser inlet velocity profile, included angle and profile. Once the throat length is given, the diffuser of smaller included angle or greater length has more uniform velocity profile at diffuser outlet. With the throat and diffuser length being set, the trumpet-shaped diffuser has nearly the same velocity profile as the conical diffuser at the diffuser outlet. All the velocity distributions get uniform at the pump outlet because of the straight pipe with length of $3D_d$ following the diffuser.

5. Conclusions

Trumpet-shaped diffuser was adopted to improve the annular jet pump performance. Based on the simulation results, the effect of the diffuser profile and included angle on pump performance and internal flow details was analyzed and some conclusions are obtained as follows:

(1)The simulation results of the RNG k-epsilon turbulence model show a better agreement with experiment data than that of the standard and the realizable k-epsilon models.

(2)The AJP with the CRVC/CRPC diffuser has better performance than the pump with conical diffuser as β =8°.

(3)The AJP with the CRPC diffuser has better performance than it with the CRVC diffuser at large flow ratio but worse at small flow ratio.

(4)The CRPC diffuser produces a linear pressure increase indeed. Both the CRPC and CRVC diffuser creature a smoother and more uniform pressure gradient than the conical diffuser.

(5) The CRVC/CRPC diffuser has nearly the same velocity profile as the conical diffuser at the diffuser outlet.

Acknowledgments

This research is financially supported by the National Natural Science Foundation of China under the Contract No. 51179134 and the Fundamental Research Funds for the Central Universities under the Contract No. 201120802020006.

Nomenclature

A	cross-sectional area [m^2]	r	radius [mm]
C_p	static pressure coefficient ($C_p=(p-p_p)/(0.5\rho v_t^2)$)	u	axis velocity [m/s]
		v	mean velocity [m/s]
D	diameter [m]	η	efficiency, ($\eta=MN$)
L	length [m]	**Subscript**	
p	static pressure [MPa]	d	discharge of the diffuser
P	total pressure [MPa]	p	driving nozzle
Q	volumetric flow rate [m^3/s]	s	suction inlet
M	flow ratio, ($M=Q_s/Q_p$)	t	throat
N	total pressure ratio, ($N=(P_d-P_s)/(P_p-P_d)$)	x	quantities at L_x, e.g., v_x, A_x and r_x

References

[1] Elger D. F., Taylor S. J. and Liou C. P., 1994, "Recirculation in an Annular-Type Jet Pump," ASME Journal of Fluids Engineering, Vol. 116, No. 4, pp. 735-740.

[2] Shimizu, Y., Nakamura, S., Kazuhara, S. and Kurata, S., 1987, "Studies of the Configuration and Performance of Annular Type Jet Pump," ASME Journal of Fluids Engineering, Vol. 109, No. 3, pp. 205-212.

[3] Long, X., Yan, H., Zhang, S. and Yao, X., 2010, "Numerical Simulation of the Influence of Throat Length on the Annular Jet Pump Performance," Journal of Drainage and Irrigation Machinery Engineering, Vol. 28, No.3, pp. 198-201.

[4] Kwon, O., Kim, M., Kwon, H. and Bae, D., 2002, "Two-Dimensional Numerical Simulations on the Performance of an Annular Jet Pump," Journal of Visualization, Vol. 5, No. 1, pp. 21-28.

[5] Henderson, F. D., 1959, "Effect of Profile and Length on the Efficiency of Pump Diffusers," Tech. Note 181, Rocket Propulsion Establishment, Westcott, UK.

[6] ESDU, 2006, "Ejectors and Jet Pumps-Design and Performance for Incompressible Liquid Flow," ESDU International Ltd, London, Data item 85032.

[7] Long, X., Yan, H., Yang, X. and Yao, X., 2010, "Investigation on the Jet Expanding in annular Jet Pump," Journal of Engineering Thermophysics, Vol. 31, SUPPL., pp. 145-148.

[8] Gazzar, M. E., Meakhail, T. and Mikhail, S., 2006, "Numerical Study of Flow Inside an Annular Jet Pump," Journal of Thermophysics and Heat Transfer, Vol. 20, No. 4, pp. 930-932.